The anastomosis angle does change the flow fields at vascular end-to-side anastomoses in vivo

Niels-Henrik Staalsen, MD, Michael Ulrich, MS, Jens Winther, MS, Erik Morre Pedersen, PhD, Thien How, PhD, and **Hans Nygaard, DMSc,**
Aarhus, Denmark, and Liverpool, United Kingdom

Purpose: **The purpose of this article was to study the influence of the anastomosis angle on the flow fields at end-to-side anastomoses in vivo.**
Methods: **Polyurethane grafts of similar internal diameter to that of the abdominal aorta (8 mm) were implanted from the suprarenal to the infrarenal level in 10 pigs. Three angles of standardized distal end-to-side anastomoses (90 degrees, 45 degrees, and 15 degrees) were studied. The anatomic position of the anastomoses was constant, the proximal outflow segment was occluded, and the flow rate through the graft was controlled. Flow visualization was accomplished by a color-flow Doppler ultrasound system.**
Results: **The angulation was reproduced within 10%. Gross hemodynamic parameters were stable, and the similarity parameters were typical for peripheral bypasses (mean Reynold's number is 424 and Womersley's parameter is 5.9). The flow fields were clearly dependent on the anastomosis angle. A zone of recirculation (approximately 5% of the flow area), extending from the toe to one diameter downstream, was found in the 45-degree and 90-degree anastomoses. No flow disturbances were detected at the toe and one diameter downstream with an anastomosis angle of 15 degrees. At the heel different recirculating flow patterns were found in the different anastomoses.**
Conclusion: **The anastomosis angle does change the flow fields at vascular end-to-side anastomoses in vivo. (J VASC SURG 1995;21:460-71.)**

Development of neointimal hyperplasia at vascular anastomoses is a well-known complication in vascular surgery.[1-4] Because of the localized nature of these lesions,[1-5] various hypotheses on the influence of local hemodynamics have been presented in the literature.[1-7] In particular, the theories that are based on the influence of low or oscillating wall shear stresses at or near the anastomoses have gained attention.[4-9] However, our knowledge of the hemodynamics at vascular anastomoses in terms of wall shear stresses and flow fields is based on studies performed in vitro[6-13] or on computer simulation.[14]

In vitro studies and computer simulation studies have reported that regions with disturbed flow are seen at the heel, the toe, and at the floor of the distal end-to-side anastomosis.[5-10,12-14] These disturbed flow regions (defined in this study as flow separation causing vortex formation, flow recirculation, and flow stagnation) correspond to those where pathologic studies have reported discrete development of neointimal hyperplasia.[1-5] Investigations have also been reported on how the flow fields, including the regions of disturbed flow, change as a function of the anastomosis angle.[7,9,10,13] However, no studies have, as yet, reported whether these flow fields are also seen in vivo.

If one accepts that neointimal hyperplasia is at least associated with hemodynamic flow disturbances, then any measures that may be taken to

From the Department of Thoracic and Cardiovascular Surgery and Institute of Experimental Clinical Research (Drs. Staalsen, Ulrich, Winther, Pedersen, and Nygaard), Skejby Sygehus, Aarhus University Hospital, the Cardiovascular Research Center (Drs. Staalsen, Pedersen, and Nygaard), Aarhus University, and the Department of Clinical Engineering (Dr. How), University of Liverpool.
Supported by The Danish Heart Foundation, "Civilingeniør F.V. Nyegaard og Hustru's Fond," "NOVO's Forskningsfond," The Danish Medical Association Research Fund, and "Karen Elise Jensens Fond."
Presented in part at the Fortieth Meeting of the American College of Angiology, Walt Disney World Village, Fla., Oct. 3-8, 1993.
Reprint requests: Niels-Henrik Staalsen, MD, Department of Thoracic and Cardiovascular Surgery, Skejby Sygehus, Aarhus University Hospital, Brendstrupgaardsvej, 8200 Aarhus N, Denmark.

0741-5214/95/$3.00 + 0 **24/1/61338**

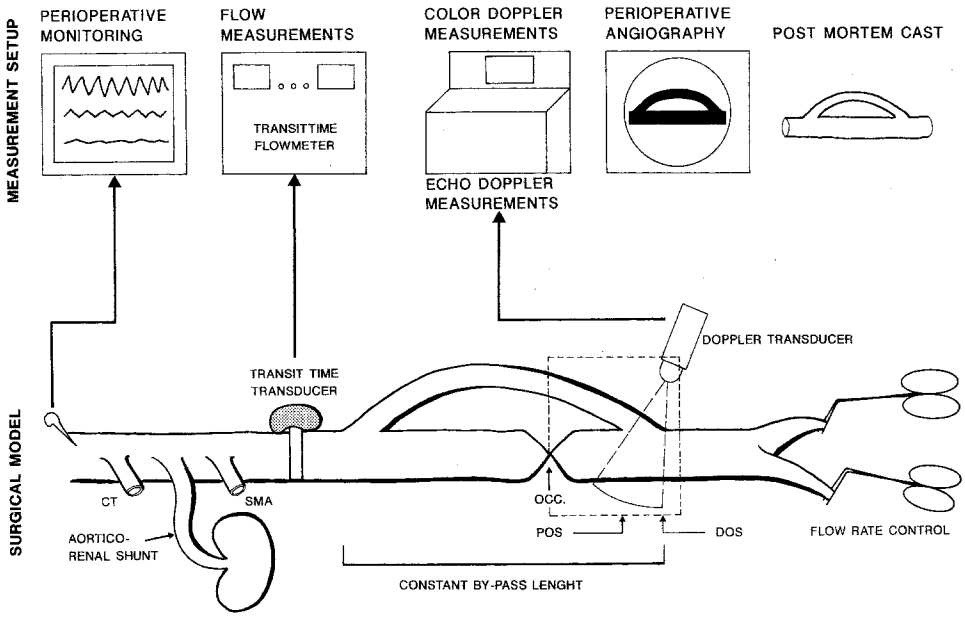

Fig. 1. Surgical model and measurement set-up. *Bottom,* Schematic drawing of abdominal aorta (all branches between superior mesenteric artery and trifurcation ligated) and bypass. *CT* represents celiac trunk, *SMA* represents superior mesenteric artery, *POS* represents proximal outflow segment, *DOS* represents distal outflow segment, *Occ.* represents occlusion of proximal outflow segment. Graft flow was adjusted by reversible clamping of iliac arteries. *Top,* Peri-operative measurement set-up.

minimize these disturbances should result in improved performance of the bypass. This study was therefore designed to investigate the flow fields at vascular anastomoses in an in vivo arterial bypass model.[15] The effect of the angle of anastomosis on the flow field was investigated with use of a color-flow Doppler scanning technique with the aim of identifying the range of angles that are associated with the least flow disturbances.

MATERIAL AND METHODS

Ten pigs (mixed Danish landrace and Yorkshire) weighing about 90 kg were used for the measurements. The care and handling of the pigs conformed with the *Guide for the Care and Use of Laboratory Animals* (NIH Publication No. 86-23) and Danish law. At the end of each study, the pig was killed by intravenous injection of saturated potassium chloride during continued anesthesia.

Anesthesia. After premedication with 4 mg/kg azeperone (Sedaparone vet); and 500 μg/kg midazolam (Dormicum); given intramuscularly, 2.5 mg/kg methomidat (Hypnodil vet); was injected intravenously. Anesthesia was maintained by 0.5% halothane, 55% nitrous oxide, and 44.5% oxygen, given through a volume-regulated ventilator (Engstrøm type ER 311; LKB Medical AB, Sweden), supplemented by continuous intravenous infusion of 1 mg/hr fentanyl (Haldid), and 23 mg/hr Dormicum. Isotonic sodium chloride (1.5 L/hr) and plasma expander (Haemaccel; 35 mg/ml/0.5 to 1.5 L) were infused throughout the experiment.

During the experiments arterial and central venous pressures were measured through liquid-filled catheters, a surface electrocardiogram was recorded, and arterial Po_2, Pco_2, pH, oxygen saturation, and hemoglobin were measured repeatedly. The animals were given an intravenous bolus injection of heparin (Leo) 40,000 IU. The activated clotting time was measured intermittently with use of a Hemachrometer (International Technidyne Corporation; Edison, N.J.) and kept above 400 seconds.

Surgical preparation. The model has been described in detail elsewhere.[15] Briefly, the abdominal aorta was dissected retroperitoneally and used for implantation of vascular grafts (electrostatically spun polyurethane grafts with an internal diameter of 8 mm and a wall thickness of 1.5 mm). All branches between the superior mesenteric artery and the aortic trifurcation were ligated, a left nephrectomy was performed, and the right kidney was perfused by a shunt supplied by the abdominal aorta proximal to the superior mesenteric artery (Fig. 1). In all pigs the toe of the proximal anastomosis was made 3 cm down-

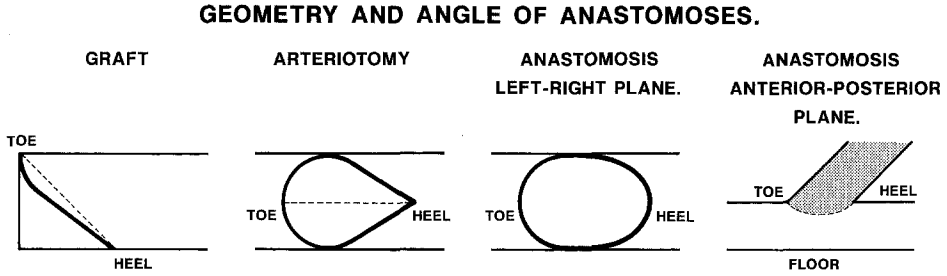

Fig. 2. Geometry and angle of anastomoses. Graft was cut from toe via half circle and extended to the heel *(solid line)*. Arteriotomy was made by vascular puncher with diameter equal to that of genuine vessel and extended to heel *(solid line)*. In this way anastomosis was made without dilation in left-right plane. In anterior/posterior plane angulation was varied by varying length toe to heel *(dotted line)*. Ninety-degree anastomosis: $L_{toe\text{-}heel}$ = 8 mm; 45-degree anastomosis: $L_{toe\text{-}heel}$ = 19 mm; 15-degree anastomosis: $L_{toe\text{-}heel}$ = 49 mm.

stream of the superior mesenteric artery, and the toe of the distal anastomosis was made 13 cm further downstream. The graft length varied according to the anastomosis angle studied: 90 degrees proximal and 90 degrees distal (graft length of 23 cm), 45 degrees proximal and 45 degrees distal (graft length of 14.5 cm), 45 degrees proximal and 15 degrees distal (graft length of 13.5 cm). The principle of the construction of the anastomosis is illustrated in Fig. 2 and described in the legend. The proximal outflow segment was ligated one vessel diameter upstream of the heel of the distal anastomosis (Fig. 1).

Anatomy. The anastomosis angle, defined as the angle between the host vessel wall and that of the graft within one vessel diameter of the anastomosis, was verified in two ways: (1) A 7.5 MHz annular phased-array transducer was used in conjunction with a Vingmed CFM 750 (Vingmed, Horten, Norway) and a commercially available software program (EchoDisp; Vingmed Sound AS, Trondheim, Norway). After two-dimensional echo Doppler measurements of the anastomosis in the anteroposterior plane, the data were stored in a Macintosh computer (Apple Computer Co., Cupertino, Calif.) and analyzed off-line (Fig. 1). (2) With a pigtail catheter positioned in the abdominal aorta via the left carotid artery and a radiographic apparatus (Model No. CB7B, Ziehm, Exposcop, Germany), perioperative contrast angiography was performed and recorded (Sony U-matic; Sony Corporation, Tokyo, Japan) for measurements of angle of anastomosis and the intraoperative dimensions of the bypass graft and the abdominal aorta (Fig. 1). To confirm the absence of a stenosis at the toe and to visualize the anastomoses three-dimensionally, a postmortem cast of the abdominal aorta and the bypass graft was made by injection of a quick-curing compound (Acrifix, Röhn GmbH, Chemische Fabrik, Germany). To ensure that the dimensions of the cast were the same as the perioperative dimensions of the bypass and the abdominal aorta, sutures were tied around the abdominal aorta at several locations before the pig was killed and the compound was injected.

Hemodynamic parameters. The flow rate was measured with a transit time flowmeter (T208, Transonic Systems Inc., New York, N.Y.), with a perivascular flow transducer placed between the proximal anastomosis and the superior mesenteric artery (Fig. 1). The flow rate was read from the flowmeter digital display, and the flow waveforms were stored in the computer by use of a commercially available software program (Flowtrace, Transonic Systems Inc.).

The flow rate was controlled by reversible cross-clamping of the iliac arteries, and the similarity parameters, mean Reynold's number, ($Re_{mean} = 2 \times Q_{mean}/(\pi \times r_{int} \times \theta)$) and Womersley's parameter ($\alpha = r_{int} \times \sqrt{2} \times \pi \times f/\theta$), were calculated from the mean flow rate (Q_{mean}) the internal radius of the graft (r_{int}), the kinematic viscosity of blood (θ), and the heart rate (f) in hertz.

Color-flow Doppler measurements. For color-flow Doppler measurements the Vingmed color-flow Doppler imaging system was used with a 7.5 MHz (Doppler frequency of 6 MHz) annular phased-array transducer, and the following measurements were obtained (Fig. 3). For all angles of distal end-to-side anastomosis, three measurement positions were chosen: the heel/graft, the toe, and one diameter downstream of the toe (1DDD). An additional measurement position, at the middle of the anastomosis, was included, when carrying out measurements in the 15-degree anastomosis. The reasons for this extra measurement position in the 15-degree anastomosis were the long distance between the toe

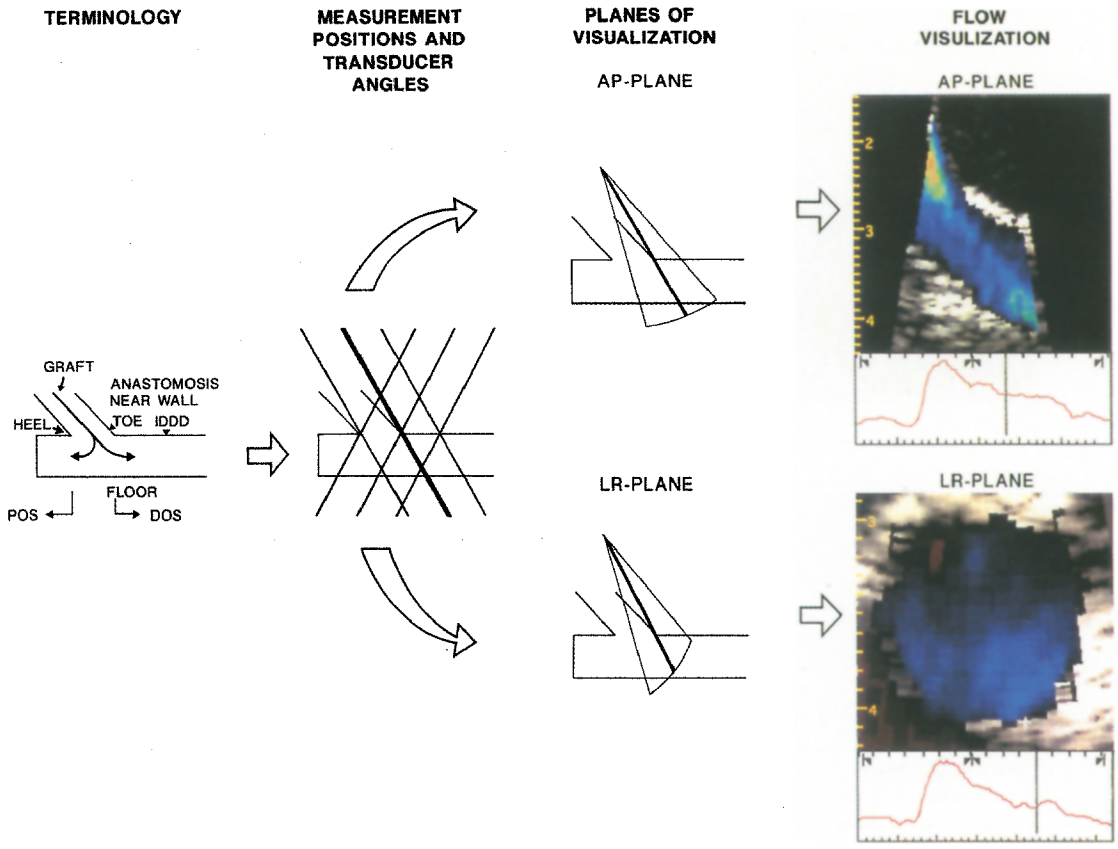

Fig. 3. Principle of color-flow Doppler measurements at distal end-to-side anastomosis, illustrated for 45-degree distal end-to-side anastomosis. *POS* represents proximal outflow segment, *DOS* represents distal outflow segment, *1DDD* represents one diameter downstream of toe of distal end-to-side anastomosis. *AP plane* represents anteroposterior plane, *LR plane* represents left-right plane.

and the heel of the anastomosis (toe-to-heel length of 49 mm) and prior knowledge of the in vivo flow field, because pilot studies in the 15-degree anastomosis revealed a large zone of flow in the reverse direction that extended from the heel to the middle of the anastomosis. Because the toe-to-heel length was much shorter in the 45-degree (toe-to-heel length of 19 mm) and 90-degree (toe-to-heel length of 8 mm) anastomoses, this extra measurement position was omitted because the flow fields in the 45-degree and 90-degree anastomoses are adequately visualized by the sector probe positions at the toe and heel measurement positions in the anteroposterior plane.

At each measurement position, the Doppler transducer was externally fixed at a predetermined angle (60 degrees in relation to the axial flow direction in the abdominal aorta), with the sector in the anteroposterior plane (Fig. 3). To visualize high velocities without aliasing errors (velocities higher than the Nyquist velocity/the color-flow Doppler can measure), the low-velocity reject (LV) was increased (range 0.10 to 0.20 m/sec) until aliasing within the color-flow Doppler image disappeared. This LV setting is a high-pass filter function, also known as "wall motion filter," which may be varied in steps on the Vingmed color-flow Doppler system. If a certain LV, for example 0.08 m/sec, is chosen, the Doppler scanner will not measure velocities in the range −0.08 to 0.08 m/sec. Velocities in that range will be visualized as black regions in the color-flow Doppler image, which in this study was used to pinpoint the low velocity zones. After recording and storing the velocity information with high LV from one heart cycle on a Macintosh computer, the measurements were repeated with a low LV setting (range 0.03 to 0.08 m/sec) so that the direction (toward the transducer = reverse velocities or away from the transducer) of the flow within the low velocity zone could be determined.

The transducer was then rotated by 90 degrees,

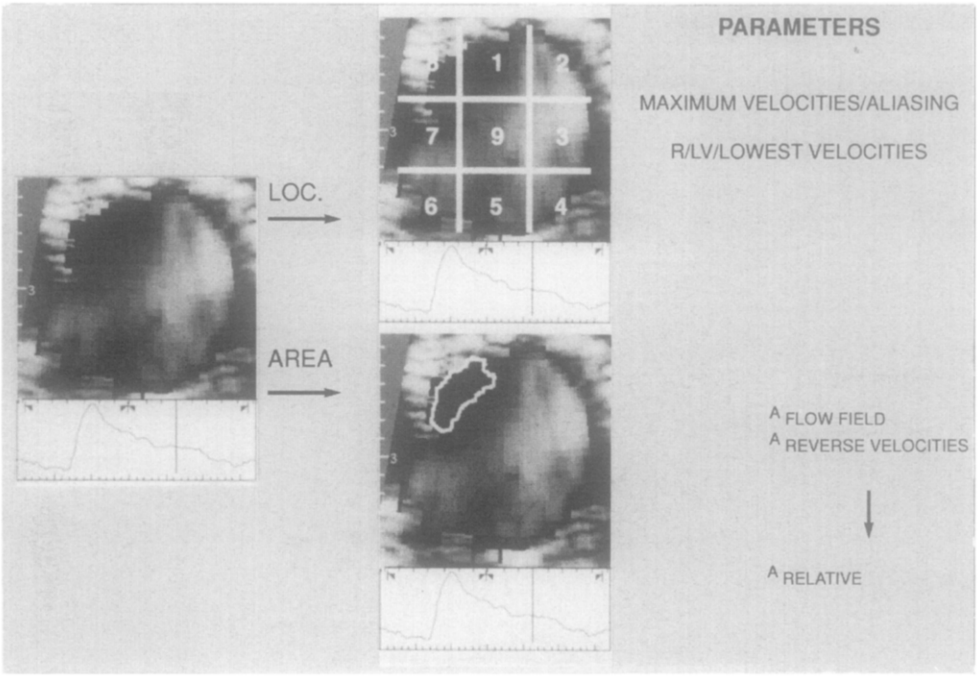

Fig. 4. Principle of data evaluation. To left, frame from late deceleration. Spatial position of maximum velocities and lowest velocities/reverse velocities were assigned number as shown in top row. Maximum velocities are thus at position 3, and lowest velocities/reverse velocities are seen at position 1. In bottom row, principle of estimating relative areas of "zones with reversed velocities" is shown. With computer software area of entire flow field was determined. With same computer program, zone with reversed flow was measured, and relative area calculated.

and the same procedures were repeated to obtain the flow field at the same measurement position in the left-right plane (LR plane) (Fig. 3). Having mapped the entire flow field, the procedures were repeated for each measurement position in the 45-degree and 15-degree anastomoses, with a fixed transducer angle of 120 degrees in relation to the longitudinal axis of the abdominal aorta. For all measurements, the Doppler sector angle that gave the maximum possible frame rate (number of color-flow Doppler pictures per second) was chosen. The quality (number of pulse trains used for Doppler velocity estimation) was left at a default setting (middle position), and the color gain was adjusted according to the procedure of Wittlich et al.,[16] whereby the gain is initially increased to its maximum value and then reduced until the noise disappears.

The beam width of this Doppler system operated in color-flow Doppler sector mode was approximately 2 mm as determined by a moving string test target.[15] The sector angle was typically either 20 or 30 degrees, the number of sector lines across the sector angle was 32 for a sector angle of 20 degrees, and 64 for an angle of 30 degrees. The number of gates along the individual sector line was 128. With these settings, the frame rate typically ranged from 20 to 40 frames/sec.

Data evaluation. During all measurements the color coding was red toward the transducer and blue away from the transducer. Images of the flow field were therefore obtained as different hues of red (bright red, high velocities; dark red, low velocities; black, velocities below the LV; and blue, velocities away from the transducer or reverse velocities) with an insonation angle of 120 degrees in relation to the axis of the abdominal aorta and as different hues of blue (bright blue, high velocities; dark blue, low velocities; black, velocities below the LV; and red, velocities toward the transducer or reverse velocities) with an insonation angle of 60 degrees.

With EchoDisp software, the downloaded data with high and low LV settings from one complete heart cycle in each measurement plane and position were visualized dynamically. The measurements in the anteroposterior plane were performed to gain information of the overall flow field in the center plane of the anastomosis, whereas the measurements in the LR plane were performed to determine the

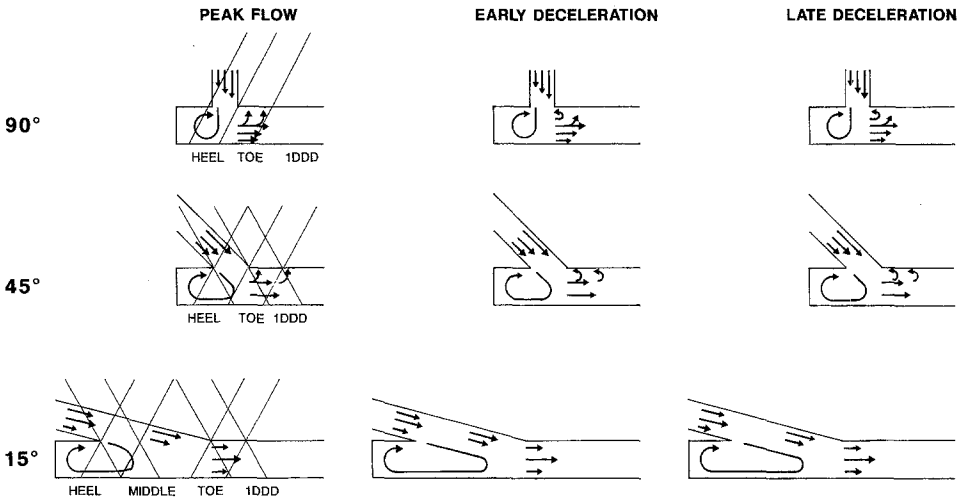

Fig. 5. Summary and interpretation of flow visualization. *Oblique lines* illustrate transducer positions and angles of insonation. **Top row** illustrates interpretation of flow field during peak flow, early and late deceleration in 90-degree anastomosis. **Middle row** illustrates same for 45-degree anastomosis. In **bottom row** interpretation of flow field in 15-degree anastomosis is shown.

spatial localization of maximum velocities and lowest velocities/velocities in the reverse direction at each measurement position.

Accordingly, a typical frame (color-flow Doppler image typical for the relevant flow phase) during the following periods of the cycle was selected: flow acceleration, peak flow, early deceleration, and late deceleration. The spatial location of the maximum velocities and of the reverse/lowest velocities was determined during that part of the flow cycle and assigned a number as illustrated in Fig. 4. This ensured that determination of the spatial location of the velocity parameters was standardized. In analysis of the data obtained with high LV, images of the spatial location of the highest velocities were obtained as the brightest hue of the color corresponding to the overall direction of flow—red with an insonation angle of 120 degrees, blue with an insonation angle of 60 degrees—and images of the lowest velocities were obtained either as black (velocities below the LV setting) or as a dark hue of the color corresponding to the overall flow direction. Zones of reverse velocities were defined as a zone with the contrast color of the color indicating the overall flow direction surrounded by black pixels (flow below the low velocity reject is LV). If no reverse velocities were detected, the position of flow below LV was indicated, and if none of the above were detected, the position of the lowest flow was obtained. To determine the direction of the velocities in the low velocity zones, the measurements in the same planes and positions with a low LV setting were analyzed in the same way. Although when this LV setting was used, the highest velocities were often aliased, which enabled the direction of velocities above the LV in the low velocity zones to be determined.

To get an overall view of the flow fields in the different anastomoses, the diagrams illustrated in Fig. 5 were constructed. These diagrams indicate the characteristics of the flow field determined from the color-flow Doppler data and show the location of the highest, the lowest, and the reverse velocities by arrows at each anatomic position at different phases of the flow cycle.

The size of the zones with reverse velocities were analyzed from the same frames in the LR plane. By determining the area of the total flow field and the area of any reverse velocity zone from the selected frame by computerized planimetry, the size of the reverse velocity zone was expressed as a percentage of the entire flow field area (Fig. 4).

RESULTS

Three pigs with a distal anastomosis angle of 90 degrees, three with an angle of 45 degrees, and four with an angle of 15 degrees were studied. A total of 236 color-flow Doppler measurements of the flow fields were performed in the different measurement positions in the 10 pigs. During these measurements, the mean flow rate (absolute minimum to absolute maximum) ranged from 0.50 to 0.74 L/min (mean of 0.62 L/min, SD 0.06), the heart rate ranged from 37

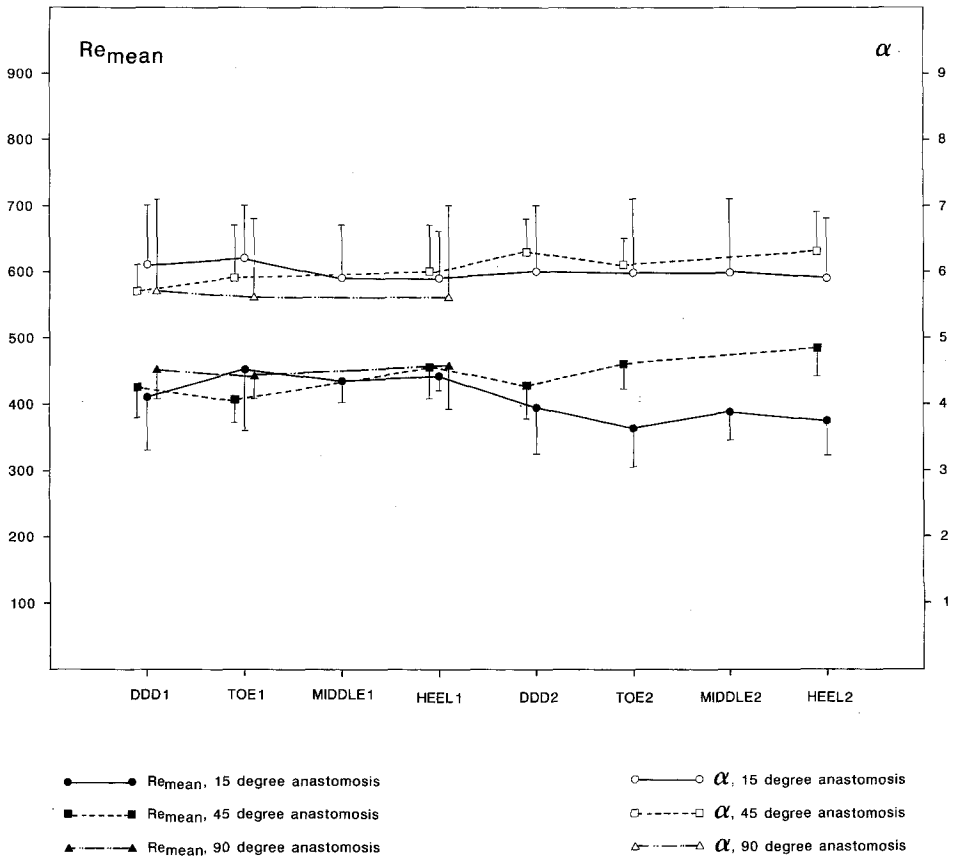

Fig. 6. Graphic presentation of stability of similarity parameters. Mean values and standard deviations for three different anastomosis angles in terms of mean Reynold's number (Re_{mean}) and Womersley's parameter (α) during measurements. $Re_{mean} = Q \times 2/(\pi \times r \times \theta)$ and $\alpha = r \times \sqrt{2} \times \pi \times f/\theta$.

Table I. Anatomic dimensions of the distal end-to-side anastomosis

No. of pigs	*Aimed angle (degrees)*	*Observed angle (degrees)*	*Relative diameters*		
			Toe	*Middle*	*Heel*
4	15	14.3 ± 1.3	1.2 ± 0.2	1.5 ± 0.2	1.2 ± 0.1
3	45	44.5 ± 3.9	1.1 ± 0.1	1.2 ± 0.1	1.2 ± 0.2
3	90	83.5 ± 3.5	1.0 ± 0.2	1.0 ± 0.1	1.0 ± 0.2

The observed angle was measured by intraoperative two-dimensional-echography and contrast angiography. Toe, middle, and heel are the diameters of the abdominal aorta at the distal anastomosis divided by the graft diameter measured by intraoperative angiography.

to 98 bpm (mean of 74 bpm, SD 21 bpm), and the mean arterial pressure ranged from 49 to 83 mm Hg (mean of 64 mm Hg, SD 12 mm Hg) for all pigs. The Re_{mean}, and α ranged from 297 to 576 (mean of 424, SD 57) and 4.0 to 7.1 (mean of 5.9, SD 0.8), respectively. The mean values and standard deviations of the different anastomosis angles are presented as a function of measurement position in Fig. 6. In Table I, the anatomic data on the observed anastomosis angle in the anteroposterior plane as measured by perioperative angiography and echo Doppler scanning and the diameters of the anastomoses in the LR plane (perioperative angiography) are presented. The 15-degree anastomosis had a slight tendency for dilation at the middle, but no dilation was identified with less obtuse angulation. The observed angles were very close to the intended angles (Table I), and no stenoses (evaluated by perioperative echo Doppler scanning and postmortem casts) were seen at the toes of the anastomoses.

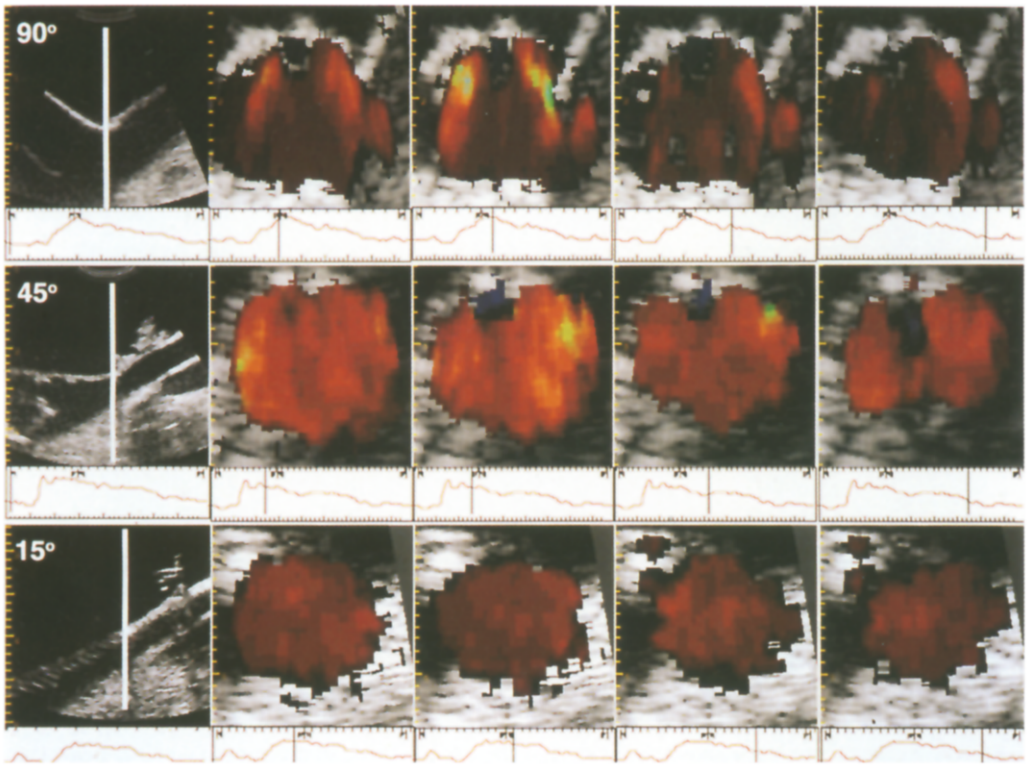

Fig. 7. Flow visualization in LR-plane at toe of 90-degree, 45-degree, and 15-degree anastomosis. Doppler probe angle is at 60 degrees (see Fig. 3). Color coding: *red* towards, *blue* away from transducer (positioned at top of image). Timing in cardiac cycle is indicated in flow tracing below each image. Typically acceleration phase did not differ between different anastomosis angles. **Top row,** Pig EC20, 90-degree anastomosis angle: First illustration shows position of transducer at toe. At near wall small zone with reverse velocities *(blue)* is fluctuating during peak flow and deceleration. **Middle row,** Pig EC13, 45-degree anastomosis angle: First illustration shows position of transducer at the toe. During early and late deceleration small zone at near wall develops. **Bottom row,** Pig EC12, 15-degree anastomosis angle: First illustration shows position of transducer at toe. During all phases no flow disturbances were seen in this position.

Flow visualization

Ninety-degree anastomosis. The main features of the flow patterns observed at peak flow and early and late deceleration are summarized diagrammatically in Fig. 5. In the graft, at the entrance of the distal end-to-side anastomosis, the highest velocities were seen at the outer wall (the graft wall that is anastomosed to the toe of the anastomosis) of the graft, and the lowest velocities occurred near the inner wall (defined as the graft wall, which is anastomosed to the heel of the anastomosis) during the entire heart cycle, indicating a skewed velocity profile. At the heel a zone of forward flow and another zone with flow either below LV or in the reverse direction were seen during deceleration. At the toe of the anastomosis (Fig. 7, *top row*) the highest velocities (bright hue of red) were seen bilaterally (in LR plane) toward the near wall at peak flow and during deceleration. As also illustrated in Fig. 7, *top row*, low velocities occurred centrally, and during deceleration flow reversal was consistently seen at the near wall. In Table II the spatial location and the estimated relative size of the reverse velocity zones during peak flow, early and late deceleration at the toe, and at 1DDD are summarized. In one pig a very large zone of reverse velocities was seen centrally (LR plane) during the entire heart cycle, but typically this zone was confined to less than 5% of the flow area. The flow field characteristics were the same at 1DDD, although these were less pronounced.

Forty-five–degree anastomosis. As in the case of the 90-degree anastomosis, the maximal velocities in the graft at the entrance of the anastomosis occurred near the outer wall during the entire heart cycle. At the heel, both forward and reverse flows were seen during deceleration. As illustrated in Fig.

Table II. Spatial and temporal localization of low velocity zones and estimation of the size of the zones with reversed flow

	Time			*Time*		
Position	*Peak*	*Early*	*Late*	*Peak*	*Early*	*Late*
90 degrees*		1 DDD			Toe	
Flow	Low-R	Low-R	Low-R	Low-R	R	R
Loc.	c-nw	c-nw	c-nw	c-nw	c-nw	c-nw
A_{rel} (%)	0-8	0-19	0-23	0-80.4	2-71.7	2-76.7
LV (cm/sec)	5-24			4-20		
45 degrees*		1 DDD			Toe	
Flow	Low-R	R	R	Low-R	R	R
Loc.	nw and fl	nw	nw	nw and fl	nw	nw
A_{rel} (%)	0-2	6.5-7	5-9	0-5	1-9	2-8
LV (cm/sec)	8-20			4-20		
15 degrees*		1 DDD			Toe	
Flow	–	–	–	–	–	–
Loc.	–	–	–	–	–	–
A_{rel} (%)	0	0	0	0	0	0
LV (cm/sec)	4-20			3-20		
15 degrees†		Middle 120 degrees			Middle 60 degrees	
Flow	R	R	R	–	R	R
Loc.	fl	fl	fl	–	fl and lat	fl and lat
A_{rel} (%)	5	31-43	32-35	0	10-15	20-25
LV (cm/sec)	3-20			5-20		

*Positioned at 1 DDD and at toe of the anastomosis.
†Positioned at the middle of the anastomosis with different transducer angles.
Time, Time in heart cycle; *Peak,* peak flow; *Early,* early deceleration; *Late,* late deceleration; *R,* reverse velocities; *Low,* lowest velocities; *Loc,* spacial localization; *c,* center; *nw,* anastomosis near wall; A_{rel}, range of pixel areas of the reversed flow as a percentage of the total flow area at a given time; *fl,* floor.

7, *middle row*, the maximum velocities were typically located either centrally/bilaterally (insonation angle of 120 degrees) or centrally toward the floor (insonation angle of 60 degrees not shown) at the toe. Low- or reverse-flow velocities were seen either at the near wall or toward the near wall (LR plane). This pattern was even more pronounced during deceleration. Reverse velocities were seen in all pigs in at least one of the two different transducer angles during both early and late systolic deceleration phases. The size of the zone of reverse velocities increased during deceleration (Table II). At peak flow, low velocities or reverse velocities were seen toward the floor of the anastomosis, with a transducer angle of 120 degrees (towards the heel of the anastomosis), which indicates that the reverse-velocity zone at the heel extended to this position. At 1DDD the reverse-velocity zone at the near wall and centrally/laterally located maximum velocities were a consistent finding during deceleration.

Fifteen-degree anastomosis. In the graft, at the entrance of the anastomosis, the maximum velocities were observed in the center, whereas the lowest velocities occurred near the inner wall. The velocity distribution was not significantly or observably skewed toward the outer wall of the graft. As indicated in Fig. 5, reverse velocities or very low velocities in either direction were seen at the heel. In the middle of the anastomosis, high forward velocities were seen near the outer graft wall during the entire heart cycle. On the floor of the anastomosis, reverse velocities were consistently observed during peak flow and deceleration regardless of angle of insonation. When the angle of insonation was changed from 120 degrees (toward the heel) to 60 degrees (toward the toe) the size of the zone with reverse velocities decreased, and reverse velocities were not seen during peak flow (Table II and Fig. 5). At the toe of the anastomosis, no zones of flow reversal were found and, as seen from Fig. 7, *bottom row*, the highest velocities were located centrally, whereas the lowest velocities occurred at the vessel wall (LR plane) during peak flow and deceleration. The same pattern was seen 1DDD of the toe.

DISCUSSION

To study the effect of the anastomosis angle on flow fields in vivo, it is a prerequisite that the geometry of the anastomoses and the bypass grafts are kept constant. Moreover, it should be ensured that the anatomic outlet conditions are similar in all cases. Therefore the anastomoses were made on a

straight vessel without any branches. The same anatomic position was used, and the bypass length was kept constant, although the curvature of the bypass differed because of the different anastomosis angles. A difference of curvature would be expected to influence the velocity profile[17,18] at the inlet of the distal end-to-side anastomosis. Because this problem will also be encountered in the clinical situation—a parabolic velocity profile at the entrance of the distal end-to-side anastomosis will not be seen in human bypasses because of insufficient inlet length—it will probably be necessary to state the anastomosis angle, as well as the toe-heel length of anastomoses, the bypass length, and the graft length in future studies. Furthermore, the proximal outflow segment was occluded, and the anastomosis technique was specially devised to ensure that the anastomosis angle could be controlled without producing a stenosis at the toe and with only slight dilation of the anastomosis (Table I).

The stability of the gross hemodynamics during the measurements was of utmost importance, because measurements on the same anastomosis were repeated in several anatomic positions and planes to get an overall view of the flow fields. Although the level of the similarity parameters differed slightly between the individual pigs, our model proved to be very stable, as indicated by an insignificant variation of the standard deviations at the different measurement positions (Fig. 6). Furthermore, it was possible to adjust the similarity parameters to values typical of peripheral arterial bypasses by means of graded occlusion of the iliac arteries. Similarity parameters, Reynold's numbers (mean) and Womersley's parameters, relevant for the study of peripheral and coronary arteries should range between 110 to 900 and 1.9 to 7.2, respectively.[19,20]

The color-flow Doppler ultrasound technique enables the entire velocity field within one heartbeat to be displayed. To optimize the flow visualization the following measures were taken: (1) the angles of insonation were constant in all measurements, (2) the same flow fields were insonated from two different transducer angles (60 and 120 degrees) in the 45-degree and 15-degree anastomoses, (3) the sector angle was narrowed as much as possible, and (4) the procedure for setting the gain[16] was standardized.

To reach the main goal, we chose the same anatomic measurement positions and the same angles of insonation at each position, regardless of anastomosis angle. Consequently, any difference in the flow fields could only be caused by the anastomosis angles and the curvature of the graft. To get some information on the influence of the different curvatures of the bypasses and the angle of the proximal anastomoses, we included a measurement position in the graft at the entrance of the distal end-to-side anastomosis. However, in these three-dimensional flow fields, the flow fields in the different positions will always be seen as by the transducer (i.e., from an angle of 60 degrees). To compensate for this, we insonated the same flow field from two different angles, and, if the same characteristics are seen in both cases, this may imply that the qualitative flow field data are reliable. In fact, the flow field characteristics of zones with reverse or low velocities at the near wall seen at the toe or at 1DDD in the 45-degree anastomoses could be reproduced. Fig. 8 illustrates this principle in a 45-degree anastomosis at 1DDD. With an insonation angle of 120 degrees *(top right)* the zone of low velocities *(black)* and reverse velocities *(blue)* are seen at the near wall, whereas the maximum velocities *(bright red)* are seen at the lateral vessel wall. Changing the insonation angle to 60 degrees, the existence of a zone with low velocities *(black)* and reverse velocities *(red)* at the near wall is verified. Because these zones were typically small—less than 5% of the flow area (Table II)—and located laterally (LR plane) toward the near wall, especially in the case of the 45-degree anastomoses, the exact positioning of the color-flow Doppler sector was of paramount importance. The reason for narrowing the sector angle (width of the sector) as much as possible was twofold: (1) to increase the time resolution and (2) to minimize the influence of the spread of insonation angles because of the width of the sector.

The interpretation of the flow visualization data was based on the assumption that a reverse velocity zone surrounded by black pixels (velocities below LV) is indicative of flow separation, and therefore part of a vortex. Accepting this assumption, a vortex is seen at the heel of a 90-degree anastomosis during peak flow and deceleration. At the toe a small vortex develops during deceleration in the center, at or toward the near wall surrounded by bilateral maximum velocities (LR plane). The same pattern was seen 1DDD, but is less pronounced (Fig. 5 and Table II). However, because the flow fields were only insonated from one transducer angle, and, to our knowledge, no in vitro studies have been performed with this angle of anastomosis, the interpretation should be judged with caution.

A vortex was also found at the heel of the 45-degree anastomoses. At the toe, a small vortex increasing during deceleration was found primarily at the near wall. The same pattern was seen 1DDD (Fig.

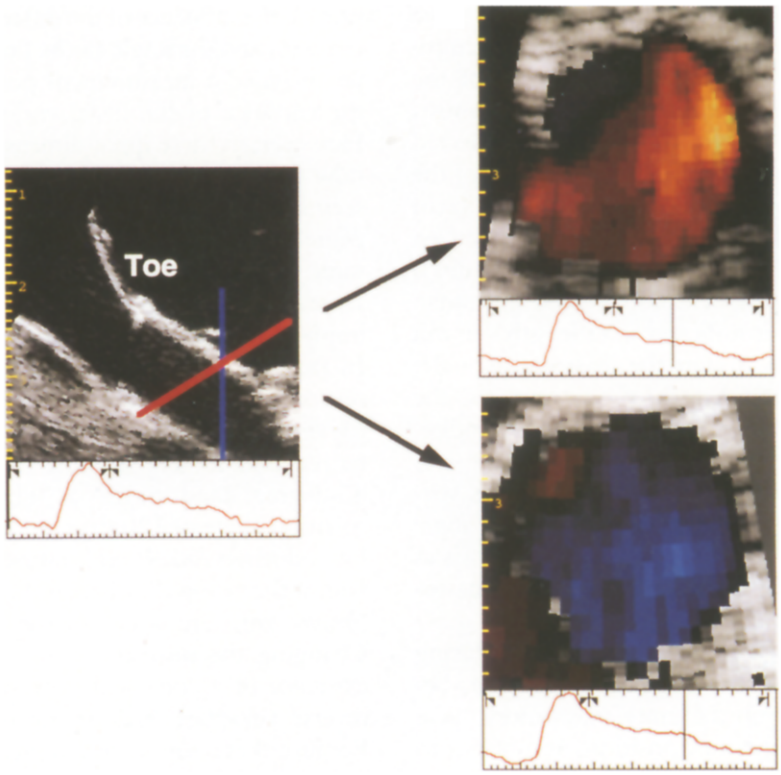

Fig. 8. Verification of presence of reverse velocities. Transducer insonates flow field at same position, 1DDD, from two different insonation angles, pig EC13. To left, two-dimensional echo image of 45-degree distal end-to-side anastomosis. *Red* and *blue* lines indicate center of color-flow Doppler sectors seen to right. In both color-flow Doppler sectors shown, color coding was *red* toward and *blue* away from transducer. Regardless of transducer angle, reverse velocities may be seen slightly to right of near wall.

5 and Table II). These are in good qualitative agreement with studies performed in vitro and from two-dimensional computer simulation studies that show a vortex at the heel of 45-degree anastomoses in both steady flow[8,9] and pulsatile flow[7,8,13] experiments and in computer simulation.[14] The small vortex that develops and oscillates about the longitudinal axis during deceleration at the toe has also been reported from in vitro studies[8,10,13] and computer simulation,[14] although not all studies[7,9] have confirmed its existence. Part of the explanation for this may be the difference in the geometry of the anatomic inlet conditions[7] emphasizing the influence of geometry on local hemodynamics.

In the 15-degree anastomoses no flow disturbances were observed at the toe or at 1DDD. At the heel and near the floor of the anastomoses, a vortex was seen pulsating along the longitudinal axis of the recipient artery during deceleration, and the relative area of this vortex seemed to increase toward the heel (Fig. 5 and Table II). The undisturbed flow field at the toe of the anastomosis is an in vivo confirmation of the observations in vitro by Crawshaw et al.,[10] who found that when the proximal outflow segment is occluded in a 15-degree anastomosis, the streamlines remain attached to the vessel walls as the fluid passed through the anastomosis.

Our study thus confirms the existence in vivo of flow disturbances at and downstream of vascular end-to-side anastomoses reported from hemodynamic in vitro studies.[6,8-10,13] Furthermore, our results also confirm that the anastomosis angle is a major determinant of the local flow fields in vivo and that, when an occluded artery segment is bypassed, the 15-degree anastomosis is preferable from a hemodynamic point of view because no flow disturbances were detected at the toe or downstream of the toe in this anastomosis. However, the clinical significance of this finding still has to be determined. Nevertheless, when the distribution of neointimal hyperplasia at the distal end-to-side anastomosis, as reported by Sottiurai et al.[2,4] and Bassiouny et al.,[5] is

viewed in relation to the flow patterns, it is seen that the sites of neointimal hyperplasia correspond with the locations of zones of low or reversed velocities. This is consistent with the theories based on the influence of local flow disturbances on development of neointimal hyperplasia at vascular end-to-side anastomoses.[4-9] Accepting that the development of neointimal hyperplasia at vascular anastomoses is indeed influenced by local flow disturbances, it may be possible to reduce this pathologic process surgically by providing a more desirable hemodynamic pattern. However, to achieve this, further quantitative in vivo studies are needed, and, on the basis of this information, longer term studies should be performed to correlate the local flow fields with the development of neointimal hyperplasia.

In conclusion the anastomosis angle has been found to be a major determinant of the local flow fields in vivo. It is shown that the 15-degree anastomosis angle is associated with the least flow disturbances at the toe and at 1DDD when the proximal outflow segment is occluded. This study confirms the in vivo existence of regions with low and reverse velocities at the preferential sites in vascular end-to-side anastomoses where neointimal hyperplasia tends to form. However, further in vivo studies are required to establish the link between flow disturbances and development of neointimal hyperplasia.

REFERENCES

1. Imparato AM, Bracco A, Kim GE, Zeff R. Intimal and neointimal fibrous proliferation causing failure of arterial reconstructions. Surgery 1972;72:1007-17.
2. Sottiurai VS, Yao ST, Flinn WR, Batson RC. Intimal hyperplasia and neointima: an ultrastructural analysis of thrombosed grafts in humans. Surgery 1983;6:809-17.
3. Sottiurai VS, Sue SL, Feinberg EL, Bringaze WL, Tran AT, Batson RC. Distal anastomotic intimal hyperplasia: biogenesis and etiology. Eur J Vasc Surg 1988;2:245-56.
4. Sottiurai VS, Yao JST, Batson RC, Sue SL, Jones R, Nakamura YA. Distal anastomotic intimal hyperplasia: histopathologic character and biogenesis. Ann Vasc Surg 1989;3: 26-33.
5. Bassiouny HS, White S, Glagov S, Choi E, Giddens DP, Zarins CK. Anastomotic intimal hyperplasia: mechanical injury or flow induced. J VASC SURG 1992;15:708-16.
6. Ojha M. Spatial and temporal variations of wall shear stress within an end-to-side arterial anastomosis model. J Biomechanics 1993;26:1377-88.
7. White SS, Zarins CK, Giddens DP, et al. Hemodynamic patterns in two models of end-to-side vascular graft anastomoses: effects of pulsatility, flow division, Reynolds number, and hood length. J Biomech Eng 1993;115:104-11.
8. Ojha M, Ethier CR, Johnston KW, Cobbold RS. Steady and pulsatile flow fields in an end-to-side arterial anastomosis model. J VASC SURG 1990;12:747-53.
9. Keynton RS, Rittgers SE, Shu MC. The effect of angle and flow rate upon hemodynamics in distal vascular graft anastomoses: an in vitro model study. J Biomech Eng 1991;113:458-63.
10. Crawshaw HM, Quist WC, Serrallach E, Valeri R, LoGerfo FW. Flow disturbance at the distal end-to-side anastomosis: effect of patency of the proximal outflow segment and angle of anastomosis. Arch Surg 1980;115:1280-4.
11. Klimach O, Chapman BL, Underwood CJ, Charlesworth D. An investigation into how the geometry of an end-to-side arterial anastomosis affects its function. Br J Surg 1984;71: 43-5.
12. Watts KC, Marble AE, Sarwal SN, Kinley CE, Watton J, Mason MA. Simulation of coronary artery revascularization. J Biomech 1986;19:491-9.
13. Rittgers SE, Bhambhani GH. Doppler color flow images of iliofemoral graft end-to-side distal anastomotic models. Ultrasound Med Biol 1993;19:257-67.
14. Steinman DA, Vinh B, Ethier CR, Ojha M, Cobbold RS, Johnston KW. A numerical simulation of flow in a two-dimensional end-to-side anastomosis model. J Biomech Eng 1993;115:112-8.
15. Staalsen NH, Pedersen EM, Ulrich M, Winther J, How TV, Hasenkam JM. An in vivo model for studying local haemodynamics at vascular end-to-side anastomoses. Eur J Vasc Surg (In press).
16. Wittlich N, Erbel R, Drexler M, Mohr-Kahaly S, Brennecke R, Meyer J. Color-Doppler flow mapping of the heart in normal subjects. Echocardiography 1988;5:157-72.
17. Peronneau PA, Hinglais JR, Xhaard M, Delouche P, Philippo J. The effects of curvature and stenosis on pulsatile flow in vivo and in vitro. In: Reneman RS, ed. Cardiovascular application of ultrasound. Belgium: 1973:204-15.
18. Hamakiotes CC, Berger SA. Flow in curved vessels, with application to flow in the aorta and other arteries. In: Liepsch DW, ed. Blood flow in large arteries: applications to atherogenesis and clinical medicine. 15th ed. Basel: Karger; 1990:227-39.
19. Stein PD, Davis D, Sabbah HN, Marzilli M. Reduction of coronary flow in the native circulation after bypass. J Thorac Cardiovasc Surg 1979;78:772-8.
20. Fitzgerald DE, O'Shaughnessy AM. Cardiac and peripheral arterial responses to isoprenaline challenge. Cardiovasc Res 1984;18:414-8.

Submitted June 27, 1994; accepted Oct. 17, 1994.